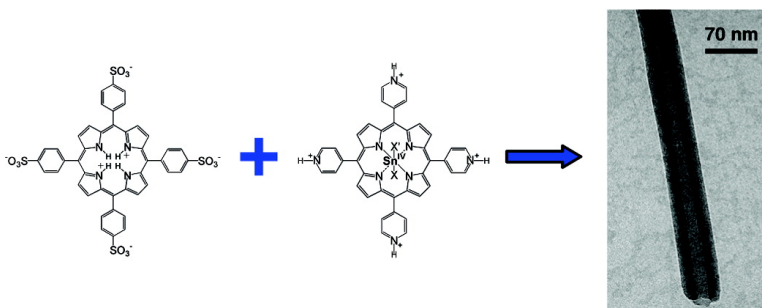


Porphyrin Nanotubes by Ionic Self-Assembly

Zhongchun Wang, Craig J. Medforth, and John A. Shelnett

J. Am. Chem. Soc., **2004**, 126 (49), 15954-15955 • DOI: 10.1021/ja045068j • Publication Date (Web): 19 November 2004

Downloaded from <http://pubs.acs.org> on April 5, 2009



More About This Article

Additional resources and features associated with this article are available within the HTML version:

- Supporting Information
- Links to the 23 articles that cite this article, as of the time of this article download
- Access to high resolution figures
- Links to articles and content related to this article
- Copyright permission to reproduce figures and/or text from this article

[View the Full Text HTML](#)

Porphyrin Nanotubes by Ionic Self-Assembly

Zhongchun Wang,^{†,‡} Craig J. Medforth,[†] and John A. Shelnutt^{*,†,§}

Biomolecular Materials and Interfaces Department, Sandia National Laboratories, Albuquerque, New Mexico 87185, Department of Chemical and Nuclear Engineering, University of New Mexico, Albuquerque, New Mexico 87131, and Department of Chemistry, University of Georgia, Athens, Georgia 30602

Received August 16, 2004; E-mail: jasheln@unm.edu

Functional self-assembled materials with well-defined shapes and dimensions are of great current interest,^{1,2} especially for applications in electronics, photonics, light-energy conversion, and catalysis. In biological systems, tetrapyrroles such as porphyrins and chlorophylls are often self-organized into nanoscale superstructures that perform many of the essential light-harvesting and energy- and electron-transfer functions. An example is the light-harvesting rods of the chlorosomes of green-sulfur bacteria, which are composed entirely of aggregated bacteriochlorophyll.^{3–6} Because of their desirable functional properties, porphyrins and other tetrapyrroles are attractive building blocks for functional nanostructures. Some synthetic porphyrins are known to form aggregates with interesting optical and electronic properties,⁷ and these aggregates sometimes occur in the form of useful nanostructures including fibers, nanorods, or thin stripes.^{8–10} However, these aggregates are more typically in less useful forms such as nanoparticles, sheets, or fractal objects.^{11,12} Thus, there is a need for well-defined and robust porphyrin nanostructures.

Here we show that robust porphyrin nanotubes can be prepared by ionic self-assembly¹³ of two oppositely charged porphyrins in aqueous solution. These sturdy nanotubes represent a new class of porphyrin nanostructures, for which the molecular building blocks (tectons) can be altered to control their structural and functional properties. The nanotubes are composed entirely of porphyrins such as those shown in Figure 1. The electrostatic forces between these porphyrin tectons, in addition to the van der Waals, hydrogen-bonding, axial coordination, and other weak intermolecular interactions that typically contribute to the formation of porphyrin aggregates, enhance the structural stability of these nanostructures.^{12,14} Molecular recognition between the complementary arrangements of opposite charges and H-bond donors and acceptors on the porphyrin tectons also contributes to the ionic self-assembly process. The porphyrin nanotubes obtained are hollow structures with uniform size and shape. They are photocatalytic, mechanically responsive and adaptive to light, and they have other interesting electronic and optical properties, some of which may mimic properties of the chlorosomal rods.

The porphyrin nanotubes are formed by mixing aqueous solutions of the two porphyrins shown in Figure 1. Typically, 9 mL of H₄TPPS₄²⁻ solution (10.5 μM H₄TPPS₄²⁻, 0.02 M HCl) was mixed with 9 mL of Sn(IV) tetrakis(4-pyridyl)porphyrin (SnTPyP²⁺) dichloride in water (3.5 μM SnTPyP²⁺), and the mixture was left undisturbed in the dark at room temperature for 72 h. Although the individual porphyrins exhibit negligible aggregation under these conditions (pH 2), the mixture of porphyrins immediately forms colloidal aggregates and, over time, provides a high yield (approximately 90%) of nanotubes (see Figure 2). The remaining 10%

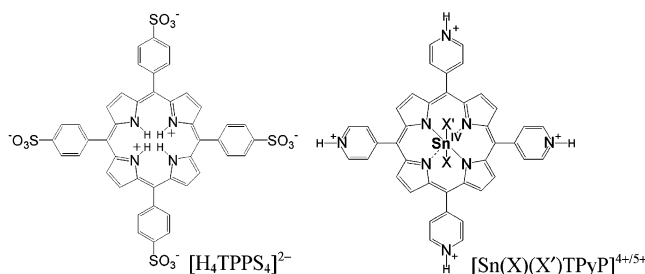


Figure 1. Porphyrins used in making the porphyrin nanotubes. The Sn(IV) center will have ligands (X, X' = Cl⁻, OH⁻, H₂O) bound above and below the porphyrin plane. At pH 2, X = OH⁻ and X' = H₂O (net charge +5) or X = X' = OH⁻ (net charge +4).

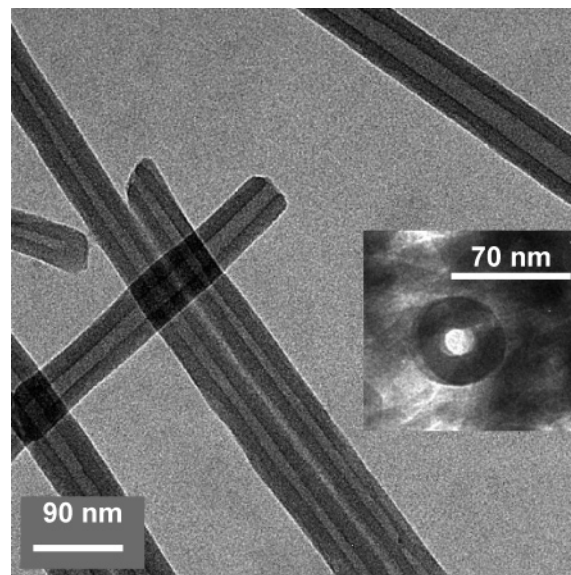


Figure 2. TEM image of the porphyrin nanotubes. (Inset) Tube trapped in a vertical orientation by a thick mat of tubes.

of the porphyrin material is mostly rodlike, with dimensions similar to those of the tubes, and thus appears to be collapsed tubes.

Transmission electron microscope (TEM) images of the porphyrin nanotubes (Figure 2 and Figures S1–S3 of the Supporting Information) reveal that they are micrometers in length and have diameters in the range of 50–70 nm with approximately 20-nm thick walls. Images of the nanotubes caught in vertical orientations (see Inset of Figure 2) confirm a hollow tubular structure with open ends. Fringes with 1.7–1.8-nm spacing are seen both in end-on views and at the edges of the nanotubes in TEM images (see Figure S1) and probably originate from the heavy tin and sulfur atoms in the porphyrin stacks. The fringes seen in the TEM images, combined with the optical spectral results discussed below, are consistent with a structure composed of stacks of offset *J*-aggregated porphyrins (individual porphyrins are approximately 2 nm × 2 nm

[†] Sandia National Laboratories.

[‡] University of New Mexico.

[§] University of Georgia.

$\times 0.5$ nm) likely in the form of cylindrical lamellar sheets. The lamellar structure would be similar to an architecture proposed for the stacking of bacteriochlorophyll molecules in the chlorosomal rods.⁴ X-ray diffraction studies (not shown) exhibit peaks in the low- and high-angle regions with line widths suggesting moderate crystallinity.

The composition of the nanotubes was determined by UV-visible absorption spectroscopy and energy-dispersive X-ray (EDX) spectroscopy. The filtered nanotubes were dissolved at pH 12, and the ratio of the porphyrins was determined by spectral simulation using extinction coefficients for $\text{H}_2\text{TPPS}_4^{4-}$ ($\epsilon_{552} = 5500 \text{ mol}^{-1} \text{ dm}^3 \text{ cm}^{-1}$) and $\text{Sn}(\text{OH})_2\text{TPyP}$ ($\epsilon_{552} = 20200 \text{ mol}^{-1} \text{ dm}^3 \text{ cm}^{-1}$), giving an approximate molar ratio of 2.4 $\text{H}_2\text{TPPS}_4^{4-}$ per $\text{Sn}(\text{OH})_2\text{TPyP}$. EDX measurements of the S:Sn atomic ratio of the porphyrin tubes on the TEM grids also indicate a molar ratio of between 2.0 and 2.5. The observed ratio of the two porphyrins in the tubes (2.0–2.5) can be related to the charges of the porphyrin species present at pH 2 (see Figure 1). As shown by acid–base titrations monitored by UV-visible spectroscopy, the porphyrin species present at pH 2 are $\text{H}_4\text{TPPS}_4^{2-}$ and a mixture of $\text{Sn}(\text{OH})_2\text{TPyP}^{4+}$ and $\text{Sn}(\text{OH})_2(\text{H}_2\text{O})\text{TPyP}^{5+}$ (formed by protonation of the pyridine substituents of $\text{Sn}(\text{OH})_2\text{TPyP}$ and, in the latter species, by the additional replacement of one OH^- axial ligand with H_2O at low pH). The formation of the nanotubes critically depends on the pH (e.g., they are not formed at pH 1 or 3), as expected, because the charge balance of the ionic tectons depends on their protonation state. EDX spectra of the nanotubes also showed no evidence of significant amounts of Cl (or I when HI was used in place of HCl), precluding the presence of chloride as counterions, axial ligands, or salt bridges. Thus far, we cannot rule out the presence of water molecules (in addition to those present as axial ligands) that might play a structural role in the nanotubes. As expected for a nanostructure formed by ionic self-assembly, the same ratio of porphyrins (2.0–2.5) is observed in the nanotubes regardless of the initial ratio of the two porphyrins in solution.

By altering the molecular structure of the porphyrin tectons, the dimensions of the nanotubes can be controlled. For example, by using Sn tetra(3-pyridyl)porphyrin instead of Sn tetra(4-pyridyl)porphyrin, nanotubes with significantly smaller average diameters were obtained (35 nm instead of 60 nm). Switching the tin porphyrins subtly repositions the charge centers and the associated H-bond donor atoms on the pyridinium rings, apparently changing the interporphyrin interactions sufficiently to alter the diameter while still allowing the tubes to form. Nanotubes are not produced when the 2-pyridyl porphyrin is used, presumably because the location of the functional nitrogen atom is changed too drastically. Axial ligation of a tecton is also important as tubes and collapsed tubes are obtained when the Sn(IV) complex is replaced with other potentially six-coordinate metal ions (e.g., Fe^{3+} , Co^{3+} , TiO^{2+} , VO^{2+}), but not when a metal that does not add axial ligands (e.g., Cu^{2+}) or the metal free porphyrin is used. These results suggest that it may ultimately be possible to achieve a high degree of control over the structure of the tubes by modifying the tectons, including variation of the peripheral substituents of the porphyrin, the metal contained in the porphyrin core, and the nature of the axial ligands.

The nanotubes exhibit some interesting and potentially useful properties. For example, the porphyrins in the nanotubes are stacked in a manner that gives UV-visible absorption bands at 496 and 714 nm that are red-shifted from the corresponding bands of the monomeric porphyrins (Figure S4a). These bands indicate formation of *J*-aggregates similar to those of $\text{H}_4\text{TPPS}_4^{2-}$ and other porphyrins,^{12,14,15} but the bands of the nanotubes are broader, suggesting the coherent coupling of the transition dipoles spans fewer

molecules than the 10–20 molecules estimated for $\text{H}_4\text{TPPS}_4^{2-}$ aggregates (Figure S4b).¹⁵ The *J*-aggregate bands of the nanotubes result in intense resonant light scattering at these wavelengths, making the nanotube suspension appear bright green under intense white light illumination, but light greenish yellow in weak transmitted light (see Figure S4, c and d). In addition, the strong fluorescence of the porphyrin monomers is almost entirely quenched in the nanotubes (data not shown).

Another potentially useful property of the nanotubes is their ability to respond mechanically to light illumination. Even though they are stable for months when stored in the dark, irradiation of a suspension of the tubes for just five minutes using incandescent light from a projector lamp ($800 \text{ nmol cm}^{-2} \text{ s}^{-1}$) results in TEM images showing rodlike structures instead of tubes. This response to light is reversible, as the tubes reform (self-heal) when left in the dark. The switch from tubular to rodlike structures in the TEM images suggests a softening of the tube walls and a collapse of the tube structure (Figure S3), perhaps as a result of photoinitiated intermolecular electron transfer that disrupts the charge balance and hence the rigidity of the structure of the ionic solid. Local heating from energy relaxation of the photoexcited porphyrin molecules might also explain the softening effect.

Further efforts are underway to characterize the optical and electronic properties of these unique nanotubes and to build functional nanoscale metal-composite devices based on the tubes using the photocatalytic properties of the Sn porphyrins in the tubes. We are also investigating how varying the structure of the porphyrin tectons leads to different nanostructures, with a goal of better understanding the ionic self-assembly process.

Acknowledgment. Sandia is a multiprogram laboratory operated by Sandia Corporation, a Lockheed-Martin company, for the United States Department of Energy under Contract DE-ACO4-94AL85000. This work was partially supported by U.S. DOE/BES Grant DE-FG02-02ER15369.

Supporting Information Available: Experimental details, UV-visible spectra, and TEM images of the nanotubes. This material is available free of charge via the Internet at <http://pubs.acs.org>.

References

- (1) Whitesides, G. M.; Mathias, J. P.; Seto, C. T. *Science* **1991**, *254*, 1312–1319.
- (2) Lehn, J.-M. *Angew. Chem., Int. Ed. Engl.* **1990**, *29*, 1304–1319.
- (3) Staehelin, L. A.; Golecki, J. R.; Fuller, R. C.; Drews, G. *Biophys. J.* **1978**, *85*, 3173–3186.
- (4) van Rossum, V.-J.; Steensgaard, D. B.; Mulder, F. M.; Boender, G. J.; Schaffner, K.; Holzwarth, A. R.; de Groot, H. J. M. *Biochemistry* **2001**, *40*, 1587–1595.
- (5) Blankenship, R. E.; Olson, J. M.; Miller, M. *Antenna Complexes from Green Photosynthetic Bacteria*; Blankenship, R. E., Madigan, M. T., Bauer, C. E., Eds.; Kluwer Academic Publishers: Dordrecht, The Netherlands, 1995; pp 339–435.
- (6) Olson, J. M. *Photochem. Photobiol.* **1998**, *67*, 61–75.
- (7) Marks, T. J. *Science* **1985**, *227*, 881–889.
- (8) Fuhrhop, J.-H.; Binding, U.; Siggel, U. *J. Am. Chem. Soc.* **1993**, *115*, 11036–11037.
- (9) Schwab, A. D.; Smith, D. E.; Rich, C. S.; Young, E. R.; Smith, W. F.; de Paula, J. C. *J. Phys. Chem. B* **2003**, *107*, 11339–11345.
- (10) Rotomskis, R.; Augulis, R.; Snitka, V.; Valiokas, R.; Liedberg, B. *J. Phys. Chem. B* **2004**, *108*, 1833–2838.
- (11) Gong, X. C.; Milic, T.; Xu, C.; Batteas, J. D.; Drain, C. M. *J. Am. Chem. Soc.* **2002**, *124*, 14290–14291.
- (12) Micali, N.; Romeo, A.; Lauceri, R.; Purrello, R.; Mallamace, F.; Scolaro, L. M. *J. Phys. Chem. B* **2000**, *104*, 9416–9420.
- (13) Faul, C. F. J.; Antonietti, M. *Adv. Mater.* **2003**, *15*, 673–683.
- (14) Lauceri, R.; Gurreri, S.; Bellacchio, E.; Contino, A.; Monsu'scolaro, L.; Romeo, A.; Toscano, A.; Purrello, R. *Supramol. Chem.* **2000**, *12*, 193–202.
- (15) Koti, A. S. R.; Taneja, J.; Periasamy, N. *Chem. Phys. Lett.* **2003**, *375*, 171–176.

JA045068J